Supporting Information

EFM data mapped into 2D images of tip-sample contact potential difference and capacitance second derivative

S.Lilliu[1,2], C.Maragliano[2], M.Hampton[1], H. Simmonds[1], M.Stefancich[2], M.Chiesa[2], M.Dahlem[2], and J. E. Macdonald[1]

[1] School of Physics and Astronomy, Cardiff University, Queens Buildings, The Parade, Cardiff CF243AA, United Kingdom

[2] Masdar Institute of Science and Technology, PO Box 54224, Abu Dhabi, United Arab Emirates

1 Linear Cantilever Physics

In order to understand the physical principles underlying tapping mode AFM and EFM tip sample interaction, a suitable model of the cantilever must be developed. In this section a complete discussion of the physics of the cantilever, readapted from Yeskin et al. [1] and Sarid et al. [2], is presented. Starting from the cantilever physics, the parabolic expression, used to relate the phase shift $\Delta\varphi$ to the applied bias V in EFM-sweep and SPP-EFM, is derived. Here the cantilever is treated as a Linear Time-Invariant (LTI) system [3, 4].

A cantilever is a beam in the form of a rectangular parallepiped having length L, thickness T ($T \ll L$), width W ($W \ll L$) and a tip with length l_{tip} at its free end (Figure 1-1). The tip-surface interaction can be schematized as a point force $\boldsymbol{F}$ applied to the tip apex (F_z normal force, F_x longitudinal force, F_y transverse force) [1]. If the tip deflection vector $\boldsymbol{r} = [x\ y\ z]$ is linearly dependent on the applied force, then the Hooke's law holds: $\boldsymbol{r} = \boldsymbol{CF}$ [1, 5]. The matrix $\boldsymbol{C}$ is the *inverse stiffness tensor* and summarizes the cantilever's elastic properties. The inverse stiffness tensor elements can be found by solving the cantilever static deformation problem under the influence of $\boldsymbol{F}$ [1]:

$$\boldsymbol{r} = \begin{bmatrix} x \\ y \\ z \end{bmatrix} = \boldsymbol{CF} = c \cdot \begin{bmatrix} \frac{2l_{tip}^2}{l^2} + \frac{t^2}{w^2} & 0 & 0 \\ 0 & \frac{3L_{tip}^2}{L^2} & \frac{3l_{tip}}{2L} \\ 0 & \frac{3l_{tip}}{2L} & 1 \end{bmatrix} \begin{bmatrix} f_x \\ f_y \\ f_z \end{bmatrix} \tag{0.1}$$

The $c_{zz} = c$ coefficient[1] is the largest one and its inverse, $K = 1/c_{zz}$, characterizes the *cantilever stiffness*. Since $\boldsymbol{C}$ is symmetric it can be diagonalised and the previous equation can be decoupled into three equations, which can be treated separately [4].

[1] $c \triangleq \frac{1}{K} \triangleq \frac{4L^3}{EWT^3} = \frac{1}{3}\frac{1}{EJ_z}L^3$ where E is the Young's modulus of the cantilever and J_z is the axial moment of inertia of the beam section about the axis that passes through its centroid.

The AFM optical system does not detect tip deflections but the inclination[2] of the cantilever's top surface near its free end [1]. By equating cantilever *strain energy* (or potential energy) when the deformation is at its maximum to the *kinetic energy,* the equation of the undamped cantilever can be obtained and the fundamental natural frequency computed (see Rayleigh and Euler-Bernoulli solutions) [1, 6].

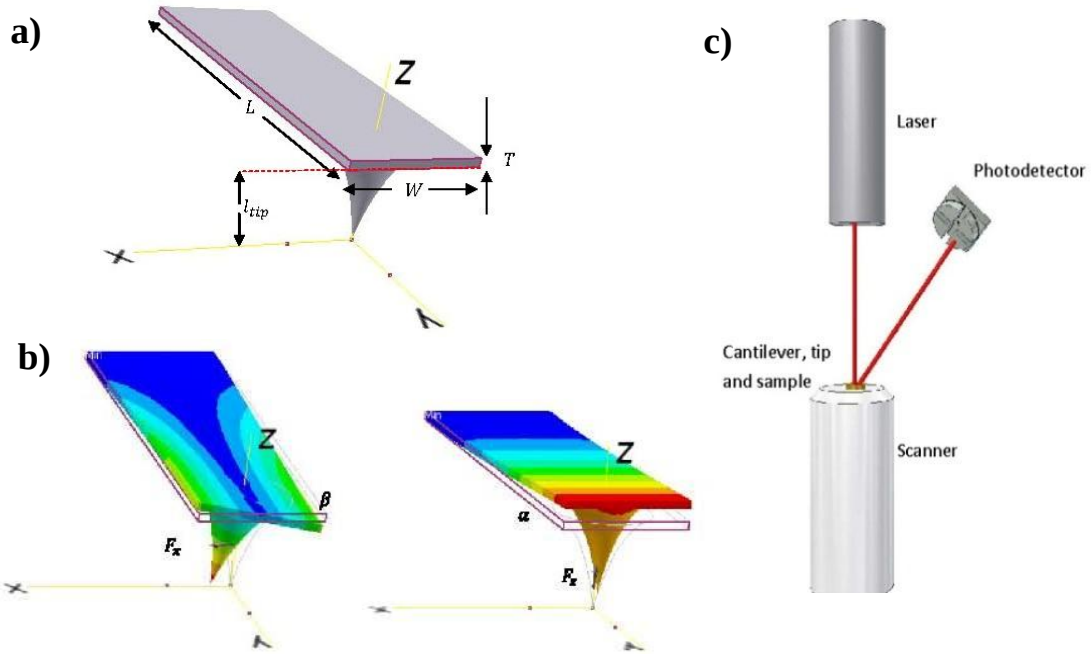

Figure 1-1 – a) Cantilever basic geometry: L is the beam length, T the beam thickness, W the beam width, l_{tip} the tip cone height. b) Angles β and α and qualitative stress analysis with Autodesk Inventor®. In colour the qualitative deformation of the cantilever (Blue: min deformation. Red: max deformation) c) Simplified description of an optical system detecting the inclination of the cantilever top surface.

In the most generic case, a generic structural system can be described by the Mass Tensor $\boldsymbol{M}$, the Stiffness Tensor $\boldsymbol{K} = \boldsymbol{C}^{-1}$, and the Damping Tensor $\boldsymbol{B}$, such that the response $\boldsymbol{r} = \boldsymbol{r}(t)$ satisfies the homogeneous equation of motion[3] [6] $\boldsymbol{M}\boldsymbol{r}'' + \boldsymbol{B}\boldsymbol{r}' + \boldsymbol{K}\boldsymbol{r} = \boldsymbol{0}$. However, since the major contribution (along z) to the cantilever vibration comes from the term $c_{z,z} = 1/K$, only the vibration with respect to the z axis ($z = u(t, L)$) is considered in the present study[4]:

$$m_{eff}u''(t,L) + Bu'(t,L) + K\,u(t,L) = 0 \text{ with } m_{eff} \approx 0.24\,m \qquad (0.2)$$

[2] Two angles are actually measured: $\begin{bmatrix}\alpha\\ \beta\end{bmatrix} = \begin{bmatrix}b_{\alpha x} & b_{\alpha y} & b_{\alpha z}\\ b_{\beta x} & b_{\beta y} & b_{\beta z}\end{bmatrix}\boldsymbol{F} = c\begin{bmatrix}0 & 3l_{tip}/l^2 & \frac{3}{2L}\\ \frac{2l_{tip}}{l^2} & 0 & 0\end{bmatrix}\boldsymbol{F}$

[3] Derived from the Rayleight solution, including the damping tensor. The $\boldsymbol{r}^n$ are time derivates.

[4] Here it is supposed that $\boldsymbol{M}, \boldsymbol{B}, \boldsymbol{K}$ are diagonal matrices so that the three equations along x, y, z can be decoupled. The u^n are time derivates.

The difference between the effective mass m_{eff} (see Rayleigh solution[5]) and the real cantilever mass is that not all the cantilever oscillates with the same amplitude. The largest deflection takes place near the free end with a decay to zero at the clamped end. The Rayleigh theory of the vibrating cantilever shows approximately the same behaviour of the Euler-Bernoulli solution evaluated at the free end of the cantilever ($y = L$), and gives approximately the same first oscillating frequency (natural frequency, $\omega_{n,1}$). If an excitation like $f(t)$ is added, it is necessary to replace the 0 in the RHS of equation (0.2) with $f(t)$. Equation (0.2) can be written in the Laplace domain [7] as $Z(s) = \mathcal{L}[z(t)], f(t) = \mathcal{L}^{-1}[F(s)]$:

$$m_{eff}s^2 Z(s) + Bs\, Z(s) + K\, Z(s) = F(s) \tag{0.3}$$

1.1 FORCED OSCILLATIONS IN THE PRESENCE OF FRICTION

The behaviour of an oscillating cantilever can be described using the model of a spring-mass-damper pendulum, which is a point mass M, suspended from a motionless support by an ideal spring having stiffness (or elastic constant) K, in a viscous medium with damping constant B. A generic force $F(s) = \mathcal{L}[f(t)]$ exciting the system is introduced. If the system is left to evolve from non-zero initial conditions, and if the energy losses are not compensated, the oscillation damps and then stops within a finite time. Using the control theory technique of the analogous circuits [8], a circuit, analogous to the mechanical system, can be used to describe the frequency response of the cantilever (Figure 1-2). The force $f(t) = \mathcal{L}^{-1}[F(s)]$ becomes a current generator, the spring becomes an inductor, the mass a capacitor, the damper a resistor. The circuit shown in Figure 1-2 is a current divider. The velocity of the mass $V_M(s) = \mathcal{L}^{-1}[v_M(t)]$ (voltage across the capacitor) is easily obtained. Using the rule of the current divider for finding the force (equivalent current) across M, and then multiplying all by the 'equivalent impedance' $1/sM$ in order to get the velocity of M (equivalent voltage):

[5] The kinetic energy is $E_k = \frac{1}{2}\left[\frac{33}{140}m\right]\left(\frac{du(t,L)}{dt}\right)^2$ and the strain (potential) energy is $E_{pot} = 3\frac{u^2(t,L)}{2L^3}EJ_z$. By differenciating the total energy dissipation $W = E_k + E_{pot}$ with respect to time, $\frac{dW}{dt} = \frac{1}{2}\left(\frac{33}{140}m\right)\frac{d^2u(t,L)}{dt^2} + \frac{1}{2}3\frac{u(t,L)}{L^3}EJ_z = 0$, which can be rewritten as $m_{eff}\frac{d^2u(t,L)}{dt^2} + K\,u(t,l) = 0$.

$$V_M(s) = \frac{F(s)}{sM}\,\frac{sM}{sM + K/s + B} = F(s)\,\frac{s}{s^2M + sB + K} \tag{0.4}$$

The displacement $Z(s)$ of the mass has to be found. Since the equilibrium position z_0 does not change, integrating $V_M(s)$ in $\mathcal{L}$ (that is multiplying by $1/s$)

$$Z(s) = \mathcal{L}[z(t)] = \frac{V_M(s)}{s} = F(s)\,\frac{1}{s^2M + sB + K} \tag{0.5}$$

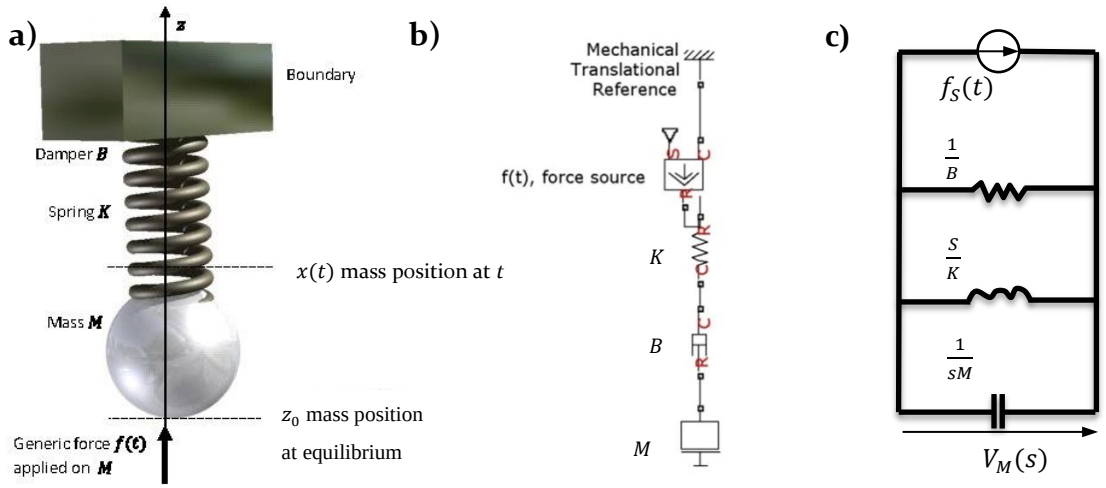

Figure 1-2 - Illustration of the spring-mass-damper pendulum (a), which represents the behaviour of the cantilever at its free end, and its relative mechanical circuit (b). Electric circuit analogous to the model of the spring-mass-damper pendulum (c).

Equation (0.5) is the same equation as the pendulum equation, $m_{eff}s^2Z(s) + Bs\,Z(s) + K\,Z(s) = F(s)$, where m_{eff} has been indicated as M. The *transfer function* [3, 7] of the linear cantilever is a second order low pass filter [9]:

$$W(s) = \frac{Z(s)}{F(s)} = \frac{1/M}{s^2 + (B/M)s + (K/M)} \tag{0.6}$$

that can be written in the Bode format [3, 4]:

$$W(s) = \frac{1}{\omega_n^2}\,\frac{1}{\frac{s^2}{\omega_n^2} + \left(\frac{1}{\omega_n Q}\right)s + 1} = \frac{1}{\omega_n^2}\,\frac{1}{\frac{s^2}{\omega_n^2} + \left(\frac{2\xi}{\omega_n}\right)s + 1} = \frac{1/K}{\frac{M}{K}s^2 + \frac{B}{K}s + 1} \tag{0.7}$$

Comparing equation (0.6) with equation (0.7) it is possible to extract the following values for the natural frequency ω_n, damping ratio ξ, quality factor Q, and the two poles (i.e. the solution of $s^2 + (B/M)s + (K/M) = 0$):

$$\omega_n = \sqrt{K/M} = \sqrt{\alpha^2 + \beta^2} \tag{0.8}$$

$$Q = \frac{K}{B}\frac{1}{\omega_n} = \frac{K}{B}\sqrt{(M/K)} = \frac{\sqrt{KM}}{B} \tag{0.9}$$

$$\xi = \frac{1}{2Q} = \frac{1}{2}\frac{B}{\sqrt{KM}} = -\frac{\alpha}{\sqrt{\alpha^2+\beta^2}} \tag{0.10}$$

$$p_1, p_2 = \alpha \pm j\beta = -\xi\omega_n \pm j\omega_n\sqrt{1-\xi^2} \tag{0.11}$$

In a normal Tapping Mode® SPM operation there are two main steps for the detection of $Z(j\omega)$ and its related quantities like the external force field: tuning of the cantilever driving frequency and surface scanning. During the tuning procedure, the cantilever is positioned far enough from the surface. The deflection of the cantilever's free end is detected by the photodetector, and a DSP allows the extraction of the $z(t)$ position. The cantilever oscillates thanks to the piezoelectric driving mechanism. A sweep of frequencies, in a reasonable range centred at the resonant frequency indicated in the datasheet of the cantilever, is done in order to obtain a plot of the $|Z(j\omega)|$ and $\arg Z(j\omega)$. After the tuning procedure one frequency of oscillation ω_0[6] is chosen. During the sample scanning, the cantilever is mechanically driven at that frequency. Once the parameters are extracted, the tip is engaged at a certain distance to the surface of the sample to analyse. This distance should be small enough in order to allow the detection of the force field $f_s(t)$. At this point, the tip oscillates because of the driving piezo mechanism and because of a force field $f_s(t)$. The new detected $\left|\tilde{Z}(j\omega_0)\right|$ and $\arg\tilde{Z}(j\omega_0)$ are extracted. By relating $Z(j\omega_0)$ and $\tilde{Z}(j\omega_0)$ useful information on f_s can be found.

The next two sections cover a discussion on the frequency response of the cantilever when the cantilever is subject to an external sinusoidal driving force (*cantilever tuning*) and when the cantilever is subject to the same external force plus a force field due to the tip-sample interaction (*surface scanning*).

[6] ω_0 indicates a generic constant frequency.

1.2 CANTILEVER TUNING: FREQUENCY RESPONSE OF THE CANTILEVER

In tapping mode the cantilever is *mechanically driven* at a frequency close to its resonant frequency. When the cantilever is far away from the sample the only force applied to the cantilever is a sinusoid. The system position is described by the transfer function $W(s) = F(s)/Z(s)$:

$$Z(s) = F(s)\frac{1}{s^2M + sB + K} \tag{0.12}$$

$$F(s) = \mathcal{L}[F \cdot sin(\omega_0 t + \varphi)] \tag{0.13}$$

where F $[N], \varphi$ [rad], ω_0[rad Hz] are constants. When the transitory period ends, the response of a stable system with respect to a sinusoidal input with constant frequency ω_0 is a sinusoidal function of the same frequency ω_0 but amplified and dephased, with respect to the input, respectively of the quantities $|W(j\omega_0)|$ and $\arg[W(j\omega_0)]$ [3]. If the system is forced with the sinusoid (0.13) with $\omega_0 = \omega_{res}$ the *asymptotic*[7] response of the system is [3]:

$$\begin{aligned} z(t) &= [|W(j\omega_{res})| \cdot F]\ sin(\omega_{res}t + \varphi + arg[W(j\omega_{res})]) \\ &= \left[\frac{1}{B\omega_n^2}\frac{1}{\sqrt{1-\xi^2}} \cdot F\right] sin\left(\omega_{res}t + \varphi + \omega_n\sqrt{(1-2\xi^2)}\right) \end{aligned} \tag{0.14}$$

The frequency response [3, 4] of this simple model can be found by substituting $s = j\omega$ in the transfer function $W(s)$. By Separating the real part from the imaginary part[8], modulus and phase are:

$$|W(j\omega)| = \frac{1}{\sqrt{(K - M\omega^2)^2 + B^2\omega^2}} \tag{0.15}$$

$$\arg[W(j\omega)] = \arctan\left(\frac{B\omega}{M\omega^2 - K}\right) \tag{0.16}$$

[7] Of course the transitory response will have another form depending on the poles of the transfer function.

[8] $\Re[W(j\omega)] = -\frac{M\omega^2 - K}{M^2\omega^4 + (B^2 - 2KM)\omega^2 + K^2}$ and $\Im[W(j\omega)] = -j\frac{B\omega}{M^2\omega^4 + (B^2 - 2KM)\omega^2 + K^2}$.
$|W(j\omega)| = \frac{1}{\sqrt{M^2\omega^4 + (B^2 - 2KM)\omega^2 + K^2}}$.

The resonant frequency is the frequency at which $|W(j\omega)|$ reaches the maximum value. By Calculating the derivative[9] of $|W(j\omega)|$, equating to zero, and solving we find[10]:

$$\omega_{res} = \omega_n \sqrt{\left(1 - \frac{1}{2Q^2}\right)} \tag{0.17}$$

$$|W(j\omega_{res})| = \frac{1}{B\omega_n} \frac{1}{\sqrt{1-\xi^2}} \tag{0.18}$$

The 3dB band of the system can be calculated by solving $|W(j\omega)|^2 = 1/2$.

1.3 Surface Scanning: Frequency Response of the Cantilever subject to a Force Field

When the cantilever is close to the sample surface, in addition to the driving sinusoidal force, an external force $f_s(z)$ acts on the system. Equation (0.12) and (0.13) become:

$$M\frac{d^2z(t)}{dt^2} + B\frac{dz(t)}{dt} + z(t)K = f(t) \tag{0.19}$$

$$f(t) = F \cdot sin(\omega_0 t + \varphi) + f_s(z(t)) \tag{0.20}$$

The term $f_s(z(t))$ is a forcing input, depending on the output $z(t)$, i.e. only on spatial coordinates. The force $f_s(z(t))$ results in a change of the position of the oscillator from the equilibrium position about which the oscillation occurs. For small oscillations the Taylor expansion of $f_s(z(t))$ around the equilibrium point z_0 is [1, 10]:

$$f_s(z(t)) = f(z_0) + \left.\frac{df_s(z(t))}{dz(t)}\right|_{z_0} \tilde{z}(t) + o\left(\tilde{z}^2(t)\right) \tag{0.21}$$

where $\tilde{z}(t) = z(t) - z_0$. This corresponds to a linear approximation of the force field. Substituting (0.21) into (0.20) and into (0.19):

---

[9] $\frac{d|W(j\omega)|}{d\omega} = -\omega(2M^2\omega^2 + B^2 - 2KM)\left(\frac{1}{M^2\omega^4 + (B^2-2KM)\omega^2 + K^2}\right)^{\frac{3}{2}}$

[10] $\omega_{res} = \frac{\sqrt{2(2KM-B^2)}}{2M} = \sqrt{\left(\frac{K}{M} - \frac{1B^2}{2M^2}\right)} = \sqrt{(\omega_n^2 - 2\alpha^2)} = \omega_n\sqrt{(1-2\xi^2)}$

$|W(j\omega_{res})| = 2(M/B)(4KM - B^2)^{-\frac{1}{2}} = 2(M/B)\frac{1}{2M}\left(\frac{K}{M} - \frac{B^2}{4M^2}\right)^{-\frac{1}{2}} = \frac{1}{B}\left(\omega_n^2 - \xi^2\omega_n^2\right)^{-1/2}$.

$$M\frac{d^2z(t)}{dt^2} + B\frac{dz(t)}{dt} + z(t)K = F \cdot sin(\omega_0 t + \varphi) + f_s(z_0) + \left.\frac{df_s(z(t))}{dz(t)}\right|_{z_0} \tilde{z}(t) + o\left(\tilde{z}^2(t)\right) \tag{0.22}$$

The equilibrium position z_0 can be easily found imposing in equation (0.21) that there is a null frequency driving the cantilever (with $\omega_0 = 0$), a null variation of $z(t)$ over the time, and a null variation of $f_s(z(t))$ over $z(t)$: $f_s(z_0) = z_0 K$. Since z_0 is a constant, the time derivatives are $\tilde{z}'(t) = z'$ and $\tilde{z}''(t) = z''$. Substituting and moving $z_0 K$ and $df_s(z(t))/dz(t)|_{z_0}\tilde{z}(t)$ in the LHS of equation (0.22) we obtain:

$$M\frac{d^2\tilde{z}}{dt^2} + B\frac{d\tilde{z}}{dt} + \tilde{z}\left[K - \left.\frac{df_s(z)}{dz}\right|_{z_0}\right] = F \cdot sin(\omega_0 t + \varphi) + o\left(\tilde{z}^2(t)\right) \tag{0.23}$$

A *new stiffness coefficient* can be defined [1]:

$$\widetilde{K} = K - \left.\frac{df_s(z)}{dz}\right|_{z_0} \tag{0.24}$$

so that

$$M\frac{d^2\tilde{z}}{dt^2} + B\frac{d\tilde{z}}{dt} + \tilde{z}\widetilde{K} = F \cdot sin(\omega_0 t + \varphi) + o\left(\tilde{z}^2(t)\right) \tag{0.25}$$

The $o\left(\tilde{z}^2(t)\right)$ can be neglected if the $f_s(z(t))$ is smooth[11] enough [1]. The forced response is $Z(s) = \widetilde{W}(s)U(s)$[12] with transfer function:

$$\widetilde{W}(s) = \frac{1/\widetilde{K}}{\frac{M}{\widetilde{K}}s^2 + \frac{B}{\widetilde{K}}s + 1} = \frac{1}{\widetilde{\omega}_n^2}\frac{1}{\frac{s^2}{\widetilde{\omega}_n^2} + \left(\frac{2\tilde{\xi}}{\widetilde{\omega}_n}\right)s + 1} \tag{0.26}$$

A perturbation in the K term perturbs also ω_0, Q, ξ and the position of the poles. The *new natural frequency* is[13]:

$$\widetilde{\omega}_n = \omega_n\sqrt{1 - \frac{1}{K}\left.\frac{df_s(z)}{dz}\right|_{z_0}} \tag{0.27}$$

where $\tilde{\xi}$ is the *new damping ratio*. The *modulus and the phase* of $\widetilde{W}(j\omega)$ are[14]:

---

[11] If its second and the higher-order derivatives are small compared to F.

[12] $\widetilde{W}(s)\left[\mathcal{L}(F \cdot sin(\omega_0 t + \varphi)) + \mathcal{L}\left[o\left(\tilde{z}^2(t)\right)\right]\right]$

[13] $\widetilde{\omega}_n = \sqrt{\frac{\widetilde{K}}{M}} = \sqrt{\frac{K}{M} - \frac{1}{M}\left.\frac{df_s(z)}{dz}\right|_{z_0}} = \sqrt{\omega_n^2 - \frac{1}{M}\left.\frac{df_s(z)}{dz}\right|_{z_0}}$

[14] $\left|\widetilde{W}(j\omega)\right| = \frac{1}{\sqrt{(\widetilde{K} - M\omega^2)^2 + B^2\omega^2}} = \frac{1}{\sqrt{M^2\omega^4 + (B^2 - 2\widetilde{K}M)\omega^2 + \widetilde{K}^2}}$

$$\left|\widetilde{W}(j\omega)\right| = \frac{1}{\sqrt{M^2\omega^4 + \left(B^2 - 2\left(K - \left.\frac{df_s(z)}{dz}\right|_{z_0}\right)M\right)\omega^2 + \left(K - \left.\frac{df_s(z)}{dz}\right|_{z_0}\right)^2}} \quad (0.28)$$

$$\arg\left[\widetilde{W}(j\omega)\right] = \arctan\left(\frac{B\omega}{M\omega^2 - \widetilde{K}}\right) = \arctan\left(\frac{B\omega}{M\omega^2 - \left(K - \left.\frac{df_s(z)}{dz}\right|_{z_0}\right)}\right) \quad (0.29)$$

The *resonant frequency* $\widetilde{\omega}_{res}$ and $\left|\widetilde{W}(j\widetilde{\omega}_{res})\right|$ are:

$$\widetilde{\omega}_{res} = \sqrt{\frac{1}{M}\left(K - \left.\frac{df_s(z)}{dz}\right|_{z_0}\right) - \frac{1B^2}{2M^2}} \quad (0.30)$$

$$\left|\widetilde{W}(j\widetilde{\omega}_{res})\right| = \frac{1}{B}\frac{1}{\sqrt{\frac{1}{M}\left(K - \left.\frac{df_s(z)}{dz}\right|_{z_0}\right) - \frac{B^2}{4M^2}}}$$

Considering the previously listed formulae, as illustrated in (0.30), if $\left.\frac{df_s(z)}{dz}\right|_{z_0} > 0$ then: $\widetilde{\omega}_{res} < \omega_{res}$; $\left|\widetilde{W}(j\widetilde{\omega}_{res})\right| > |W(j\omega_{res})|$; $\arg\left[\widetilde{W}(j\omega)\right] < \arg[W(j\omega)]$. If $\left.\frac{df_s(z)}{dz}\right|_{z_0} < 0$ then: $\widetilde{\omega}_{res} > \omega_{res}$; $\left|\widetilde{W}(j\widetilde{\omega}_{res})\right| < |W(j\omega_{res})|$; $\arg\left[\widetilde{W}(j\omega)\right] > \arg[W(j\omega)]$.

This is illustrated in Figure 1-3.

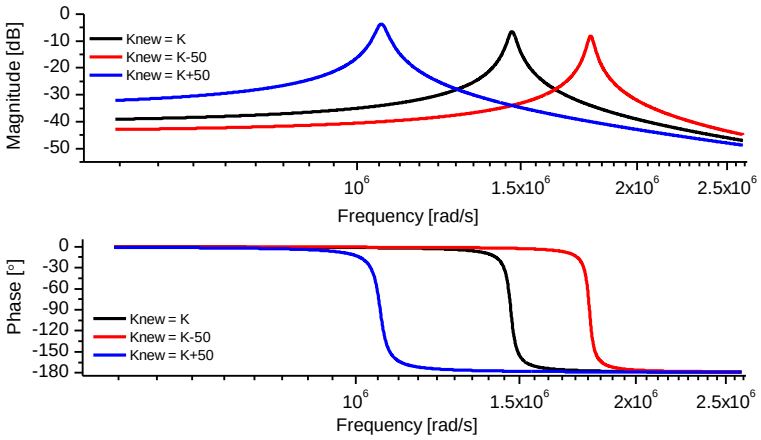

Figure 1-3 - Effect of the sign of the first derivative of the field force on the frequency response with respect to the frequency response without field force. Cantilever parameters: K= 105 Pa m, M=48.74×10^{-12}, Q=50, $df_s(z)/dz$=±50.

1.4 Detection of the External Force $f_s(z)$

By relating $W(j\omega_0)$ and $\widetilde{W}(j\omega_0)$ useful information on f_s can be found. There are several ways to extract information about f_s. Here only the phase shift is discussed because it is relevant in the EFM technique. The phase shift between $W(j\omega)$ and $\widetilde{W}(j\omega_0)$ at the natural frequency ω_n is (see (0.16) and (0.29))[15]:

$$\Delta\varphi = \left\{\arg\left[\widetilde{W}(j\omega)\right] - \arg[W(j\omega)]\right\}\Big|_{\omega=\omega_n} = \arg\left[\frac{\widetilde{W}(j\omega)}{W(j\omega)}\right]\Bigg|_{\omega=\omega_n} \tag{0.31}$$

$$\arg[W(j\omega)]|_{\omega=\omega_n} = \arctan\left(\frac{B\omega}{M\omega^2 - K}\right)\Big|_{\omega=\omega_n} = \arctan\left(\frac{B\sqrt{\frac{K}{M}}}{\frac{MK}{M} - K}\right) = \frac{\pi}{2} \tag{0.32}$$

$$\arg\left[\widetilde{W}(j\omega)\right]\Big|_{\omega=\omega_n} = \arctan\left(\frac{B\sqrt{\frac{K}{M}}}{\left.\frac{df_s(z)}{dz}\right|_{z_0}}\right) \tag{0.33}$$

Using

$$a = \frac{B\sqrt{\frac{K}{M}}}{\left.\frac{df_s(z)}{dz}\right|_{z_0}} = \frac{K/Q}{\left.\frac{df_s(z)}{dz}\right|_{z_0}} \tag{0.34}$$

the phase shift can be written as:

$$\Delta\varphi = \left\{\arg\left[\widetilde{W}(j\omega)\right] - \arg[W(j\omega)]\right\}\Big|_{\omega=\omega_n} = \arctan(\mathrm{a}) - \frac{\pi}{2} \tag{0.35}$$

Using the trigonometric relationship $\arctan(a) = -\arctan\left(\frac{1}{a}\right) + \frac{\pi}{2}$, it follows that:

$$\Delta\varphi = -\arctan\left(\frac{1}{a}\right) + \frac{\pi}{2} - \frac{\pi}{2} = -\arctan\left(\left.\frac{df_s(z)}{dz}\right|_{z_0}\frac{Q}{K}\right) \tag{0.36}$$

The force derivative can be written as:

$$\left.\frac{df_s(z)}{dz}\right|_{z_0} = -\tan\left(\frac{K}{Q}\Delta\varphi\right) \tag{0.37}$$

[15] $\widetilde{W}(j\omega)\big|_{\omega=\omega_n} = \frac{B\omega}{M\omega^2 - \left(K - \left.\frac{df_s(z)}{dz}\right|_{z_0}\right)} = \frac{B\sqrt{\frac{K}{M}}}{\frac{MK}{M} - \left(K - \left.\frac{df_s(z)}{dz}\right|_{z_0}\right)} = \frac{B\sqrt{\frac{K}{M}}}{\left.\frac{df_s(z)}{dz}\right|_{z_0}}$

Lei et al. [11] introduce further simplifications. If $a \gg 1$ (see (0.34)) is satisfied, using some trigonometric relationship we have[16]: $\arctan(a) \approx -\arcsin\left(\frac{1}{a}\right) + \frac{\pi}{2}$. Substituting in the (0.35) the same formula used by Lei et al. [11] is obtained:

$$\Delta\varphi = -\arcsin\left(\left.\frac{df_s(z)}{dz}\right|_{z_0} \frac{Q}{K}\right) \tag{0.38}$$

The force derivative can be written as:

$$\left.\frac{df_s(z)}{dz}\right|_{z_0} = -\sin\left(\frac{K}{Q}\Delta\varphi\right) \tag{0.39}$$

A further approximation can be done considering that, if $a \gg 1$, the arctan() can be expanded with the Taylor formula[17]:

$$\begin{aligned}\Delta\varphi = \left\{\arg\left[\widetilde{W}(j\omega)\right] - \arg[W(j\omega)]\right\}\Big|_{\omega=\omega_n} &= \arctan(a) - \frac{\pi}{2} \\ = \left(\frac{\pi}{2} - \frac{1}{a} + \frac{1}{3a^3} - \cdots\right) - \frac{\pi}{2} &= -\left.\frac{df_s(z)}{dz}\right|_{z_0} \frac{Q}{K}\end{aligned} \tag{0.40}$$

The force derivative can be written as:

$$\left.\frac{df_s(z)}{dz}\right|_{z_0} = -\left(\frac{K}{Q}\Delta\varphi\right) \tag{0.41}$$

This formula is used for the EFM-sweep and SPP-EFM discussion in the paper.

[16] $\sqrt{a^2+1} \approx a$, which is valid if $a^2 \gg 1$.

[17] see [12] for the formula. There are two Taylor expansions: one for $a < 1$ and onother for $a > 1$.

2 SPP-EFM: extra information

As discussed in the paper, in order to easily access the pins inside the Multimode AFM base, an extension of wires from the pins to outside the base ending with six connectors was made. A coaxial cable connected the pins to a 33220A 20Mhz Arbitrary Waveform Generator (Agilent, USA). A scheme of the setup is shown in Figure 2-1.

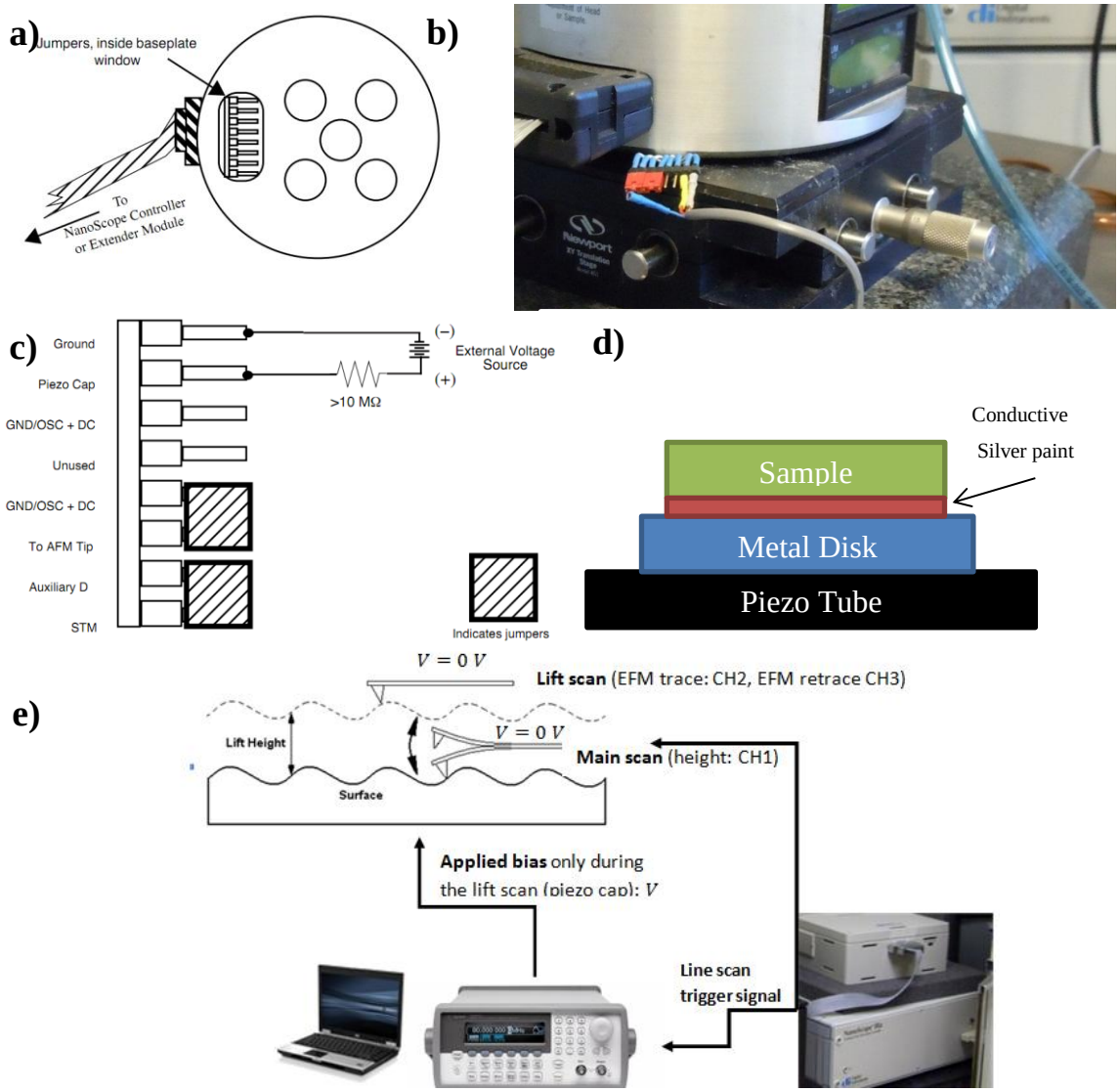

Figure 2-1 - a) Jumpers inside the baseplate of the Nanoscope III. c) Baseplate and extension for an easy access to the pins (the cable is connected to ground and piezo cap). c) Channels that can be accessed through the pins. d) Example of sample preparation. e) Setup description and applied bias scheme. Three channels are recorded: height in tapping mode, EFM-phase in lift-mode (trace and retrace). A bias is applied only during the lift mode, using an Agilent waveform generator triggered by the Nanoscope III controller. The voltages applied during the trace and retrace in EFM mode were 5×[0.5, -1, -0.75, 0] V and 5×[1, -0.5, 0.25, 0.75] V, respectively.

The waveform period must be calculated according to the AFM scan rate, and according to the fact that each segment must correspond to the appropriate line scan as discussed above[18]. Typical values are summarized in
Figure 2-1. In most of the scans shown here a scan rate[19] of 1 Hz was used. The waveform maximum amplitude was set to ± 5 V, in order to have a perfectly parabolic relationship

The SPP-EFM deconvolution scheme has already been discussed in the paper. Each step involves a parabolic fitting with the MATLAB function `fit` [13]. The function fits data in the column vectors `xdata`, represented by the applied bias, and `ydata`, represented by the measured EFM-phase signals. The fit function was assigned to a *fit object* `ft_` with the function `fittype` in the form of '`a*(x-b)^2`'. Coefficient starting points and coefficient boundaries were also assigned to `ft_`. The algorithm for the minimisation of the least squares objective function [13] was automatically selected by the `fit` function. The `fit` function returns three objects: `[cfun,gof,output]`. The first object, `cfun`, contains the optimized coefficients `a` and `b` that minimize the error function defined by the selected optimization algorithm, and their 95% confidence bounds, which are used for the construction of the dotted graphs in Figure 4 of the paper. The second object, `gof`, contains goodness-of-fit statistics. In our case, a *good fit* is defined as a model in which the model coefficients can be estimated with little uncertainty [13]. The methods for judging the quality of the fit can be graphical or numerical. Plotting residuals and prediction bounds are graphical methods that help visual interpretation, while computing goodness-of-fit statistics and coefficient confidence bounds yield numerical measures that aid statistical reasoning [13]. The object `gof` contains the following goodness-of-fit statistics: the sum of squares due to error (SSE), r-square (R^2), adjusted r-square, root mean squared error (RMSE) [13]. The SSE measures the total deviation of the response values from the fit to the response values: $SSE = \sum_{i=1}^{n}(y_i - \tilde{y}_i)^2$, where y_i are the `ydata` elements, and $\tilde{y}_i$ are the values of the fitting

[18] The waveform must be triggered first, then the tip can be engaged in lift mode. The scan will start from the middle of the image and it will be possible to start to save the image only when the tip will reach the 512 line scan.
[19] When the 4 segments waveform is used scan rates of 0.5, 1, 1.95 Hz would correspond to waveform periods of 15.99, 7.99, 4.04 s respectively. The waveform was synchronised with the scan lines using a *start phase* of +23°.

function in correspondence of the `xdata` elements [13]. A value closer to 0 indicates that the model has a smaller random error component [13]. The R^2 measures how successful the fit is in explaining the variation of the data [13]. Put another way, R^2 is the square of the correlation between the response values and the predicted response values [13]. It is also called the square of the multiple correlation coefficient and the coefficient of multiple determination. R^2 is defined as [13]:

$$R^2 = \frac{\sum_{i=1}^{n}(\tilde{y}_i - \bar{y})^2}{\sum_{i=1}^{n}(y_i - \bar{y})^2} = 1 - \frac{SSE}{\sum_{i=1}^{n}(y_i - \bar{y})^2} \tag{0.42}$$

where $\bar{y}$ is the mean of the observed data. R^2 can take on any value between 0 and 1, with a value closer to 1 indicating that a greater proportion of variance is accounted for by the model [13]. For example, an R^2 value of 0.90 means that the fit explains 90% of the total variation in the data about the average [13]. In the present work the R^2 was selected as a synthetic statistical parameter for the evaluation of the goodness-of-fit of the deconvolution procedure [13]. It is worth observing that the 95% confidence bounds, Δa and Δb are also used for the generation of extra channels defined as the relative errors $\varepsilon_a = \Delta a/a$ and $\varepsilon_b = \Delta b/b$. Finally, the third object, `output`, contains information associated with the fitting algorithm. In this case, the selected algorithm for the minimization of the objective function was the *Trust-Region Reflective Newton* [13].

References

[1] I.N. Yeskin, SPM Basics, 2005, http://www.ntmdt.com/spm-basics/view/sfm.
[2] D. Sarid, Scanning Force Microscopy, Oxford University Press, 1991, 9789512292219.
[3] Ferrante A., Lepschy A., V. U., Introduzione ai controlli automatici, CittàStudi, 2008, 8825173350.
[4] A. Giua, C. Seatzu, Analisi dei Sistemi Dinamici, Springer, 2006, 8847002842.
[5] R.P. Feynman, R.B. Leighton, M. Sands, The Feynman Lectures on Physics, Addison-Wesley Publishing Company Inc., 0805390456.
[6] D.F. Pilkey, Computation of a Damping Matrix for Finite Element Model Updating Engineering Mechanics, Virginia Polytechnic Institute and State University, PhD Thesis, Blacksburg, 1998, pp. 128.
[7] M. Codegone, Metodi Matematici per l'Ingegneria, Zanichelli, 1995, 8808098141.
[8] J.J. D'Azzo, C.H. Houpis, Feedback control system analysis and synthesis, 1966, 0070161755
[9] A.S. Sedra, K.C. Smith, Microelectronic circuits, 5th ed., Oxford University Press, 2004, 0195142519.
[10] J.J.E. Splotine, W. Li, Applied Nonlinear Control, Prentice-Hall, 1991.
[11] C.H. Lei, A. Das, M. Elliott, J.E. Macdonald, Quantitative electrostatic force microscopy-phase measurements, Nanotechnology, (2004) 627.
[12] A. Bruce Carlson, Paul B. Crilly, J.C. Rutledge, Communication Systems: An Introduction to Signals and Noise in Electrical Communication, 4th ed., McGraw-Hill Higher Education, 0070111278.
[13] MATLAB, Matlab User Guide, 2011, http://www.mathworks.co.uk/help/techdoc/index.html.